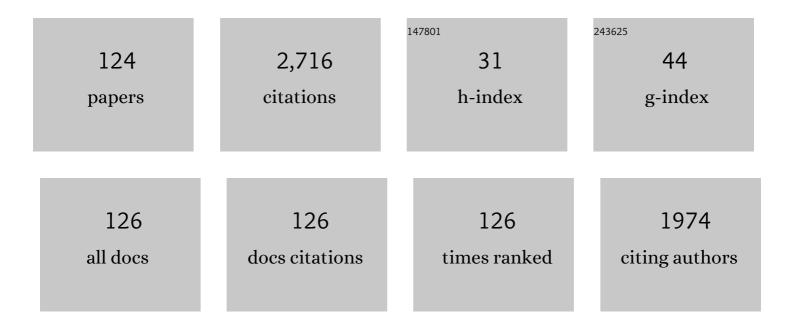
List of Publications by Year in descending order

Source: https://exaly.com/author-pdf/3580997/publications.pdf Version: 2024-02-01



#	Article	IF	CITATIONS
1	Plug and Play Electrodeposition Cell: A Case Study of Bismuth Ferrite Thin Films for Photoelectrochemical Water Splitting. ECS Journal of Solid State Science and Technology, 2022, 11, 013006.	1.8	2
2	Role of Laser Excitation Wavelength and Power in the Fano Resonance Scattering in RFe <sub>0.50</sub> Cr <sub>0.50</sub> O <sub>3</sub> ( <i>R</i> = Sm, Er, and Eu): A Brief Raman Study. Journal of Physical Chemistry C, 2022, 126, 5403-5410.	3.1	13
3	Investigating the structural, vibrational, optical, and dielectric properties in Mg-substituted LaAlO3. Journal of Materials Science: Materials in Electronics, 2022, 33, 13352-13366.	2.2	5
4	Probing the effect of R-cation radii on structural, vibrational, optical, and dielectric properties of rare earth (R=La, Pr, Nd) aluminates. Ceramics International, 2022, 48, 23072-23080.	4.8	8
5	Correction to "Role of Laser Excitation Wavelength and Power in the Fano Resonance Scattering in RFe <sub>0.50</sub> Cr <sub>0.50</sub> O <sub>3</sub> ( <i>R</i> = Sm, Er, and Eu): A Brief Raman Studyâ€ Journal of Physical Chemistry C, 2022, 126, 10618-10619.	3.1	0
6	Temperature-dependent dielectric loss in BaTiO3: Competition between tunnelling probability and electron-phonon interaction. Materials Chemistry and Physics, 2021, 257, 123792.	4.0	25
7	Doping-Induced Combined Fano and Phonon Confinement Effect in La-Doped CeO <sub>2</sub> : Raman Spectroscopy Analysis. Journal of Physical Chemistry C, 2021, 125, 2648-2658.	3.1	43
8	Possibility of relaxor-type ferroelectricity in delafossite CuCrO2 near room temperature. Solid State Sciences, 2021, 112, 106509.	3.2	4
9	Electronic and optical properties of Y-doped \$\$hbox {BaBiO}_{3}\$\$. European Physical Journal B, 2021, 94, 1.	1.5	0
10	Unorthodox Approach to Realize the Correlation between the Dielectric Constant and Electronic Disorder in Cr-Doped PrFeO <sub>3</sub> . Journal of Physical Chemistry C, 2021, 125, 7378-7383.	3.1	20
11	Origin of ferroelectricity in cubic phase of Hf substituted BaTiO <sub>3</sub> . Journal of Physics Condensed Matter, 2021, 33, 165403.	1.8	15
12	Structural, optical and dielectric properties of Bi substituted polycrystalline praseodymium chromate. Materials Chemistry and Physics, 2021, 262, 124313.	4.0	10
13	New route to estimate the Mott-Hubbard and charge transfer parameters: An optical and x-ray absorption studies. Solid State Sciences, 2021, 115, 106582.	3.2	16
14	Investigations on the Electronic Structure of the Strongly Correlated Electron System Cr-Doped PrFeO <sub>3</sub> . Journal of Physical Chemistry C, 2021, 125, 14048-14055.	3.1	7
15	Possibility of using ultraviolet radiation for disinfecting the novel COVID-19. Photodiagnosis and Photodynamic Therapy, 2021, 34, 102234.	2.6	22
16	Distorted octahedra induced anisotropic strain and local disorder in delafossite CuCrO2. Solid State Sciences, 2021, 117, 106602.	3.2	3
17	Origin of natural and magnetic field induced polar order in orthorhombic PrFe1/2Cr1/2O3. Physical Review B, 2021, 104, .	3.2	14
18	Reply to the comment on Kumar A., Sagdeo A., Sagdeo P. R., Possibility of using ultraviolet radiation for disinfecting the novel COVID-19, Photodiagnosis and photodynamic therapy. 34 (2021) 102234. Photodiagnosis and Photodynamic Therapy, 2021, 35, 102419.	2.6	0

#	Article	IF	CITATIONS
19	Effect of Ca substitution on structural and optical properties of multiferroic PrCrO3. AIP Conference Proceedings, 2021, , .	0.4	0
20	Structural, magnetic and electronic properties of Zn0.94Co0.06O/ZnO heterostructure. Applied Physics A: Materials Science and Processing, 2021, 127, 1.	2.3	0
21	Exploring the Interrelation between Urbach Energy and Dielectric Constant in Hf-Substituted BaTiO <sub>3</sub> . ACS Omega, 2021, 6, 32231-32238.	3.5	50
22	Investigating the correlation between the Urbach energy and asymmetry parameter of the Raman mode in semiconductors. Physical Review B, 2021, 104, .	3.2	15
23	Comparative structural and optical studies on pellet and powder samples of BaTiO3 near phase transition temperature. Ceramics International, 2020, 46, 3250-3256.	4.8	19
24	Cluster Glass Behavior in Orthorhombic SmFeO <sub>3</sub> Perovskite: Interplay between Spin Ordering and Lattice Dynamics. Chemistry of Materials, 2020, 32, 1250-1260.	6.7	27
25	Structural and optical properties of transparent, tunable bandgap semiconductor: α-(AlxCr1â^'x)2O3. Journal of Applied Physics, 2020, 128, 135703.	2.5	1
26	Effect of bismuth doping on optical properties of polycrystalline PrCrO3. AIP Conference Proceedings, 2020, , .	0.4	6
27	The magneto-elastic and optical properties of multiferroic GaFeO3-δ. Journal of Magnetism and Magnetic Materials, 2020, 514, 167210.	2.3	19
28	Structural, optical, and dielectric investigations in bulk PrCrO3. Journal of Materials Science: Materials in Electronics, 2020, 31, 16379-16388.	2.2	6
29	Improved analytical framework for quantifying field emission from nanostructures. Materials Chemistry and Physics, 2020, 245, 122686.	4.0	8
30	Orbital facilitated charge transfer originated phonon mode in Crâ€substituted PrFeO <sub>3</sub> : A brief Raman study. Journal of Raman Spectroscopy, 2020, 51, 1210-1218.	2.5	22
31	Enhancing Viologen's Electrochromism by Incorporating Thiophene: A Step Toward Allâ€Organic Flexible Device. Physica Status Solidi (A) Applications and Materials Science, 2019, 216, 1800680.	1.8	18
32	Design and development of a fully automated experimental setup for <i>in situ</i> temperature dependent magneto-dielectric measurements. Measurement Science and Technology, 2019, 30, 125901.	2.6	10
33	Charge neutral crystal field transitions: A measure of electron–phonon interaction. Journal of Physics and Chemistry of Solids, 2019, 135, 109102.	4.0	18
34	Optical spectroscopy: An effective tool to probe the origin of dielectric loss in Cr doped PrFeO3. Ceramics International, 2019, 45, 8585-8592.	4.8	29
35	Effect of self-doping on the charge state of Fe ions and crystal field transitions in YFeO3: Experiments and theory. Journal of Applied Physics, 2019, 125, .	2.5	22
36	Prussian Blue-Viologen Inorganic–Organic Hybrid Blend for Improved Electrochromic Performance. ACS Applied Electronic Materials, 2019, 1, 892-899.	4.3	56

#	Article	IF	CITATIONS
37	Deconvoluting Diffuse Reflectance Spectra for Retrieving Nanostructures' Size Details: An Easy and Efficient Approach. Journal of Physical Chemistry A, 2019, 123, 3607-3614.	2.5	13
38	Strain induced disordered phonon modes in Cr doped PrFeO <sub>3</sub> . Journal of Physics Condensed Matter, 2019, 31, 275602.	1.8	31
39	Direct correlation between the band gap and dielectric loss in Hf doped BaTiO3. Journal of Materials Science: Materials in Electronics, 2019, 30, 8064-8070.	2.2	25
40	Possible evidence of delocalized excitons in Cr-doped PrFeO3: An experimental and theoretical realization. Journal of Physics and Chemistry of Solids, 2019, 130, 230-235.	4.0	17
41	Effect of structural disorder on the electronic and phononic properties of Hf doped BaTiO3. Journal of Materials Science: Materials in Electronics, 2019, 30, 9498-9506.	2.2	33
42	Investigation of temperature-dependent optical properties of TiO2 using diffuse reflectance spectroscopy. SN Applied Sciences, 2019, 1, 1.	2.9	45
43	Precursor concentration dependent hydrothermal NiO nanopetals: Tuning morphology for efficient applications. Superlattices and Microstructures, 2019, 125, 138-143.	3.1	26
44	Polythiophene–PCBM-Based All-Organic Electrochromic Device: Fast and Flexible. ACS Applied Electronic Materials, 2019, 1, 58-63.	4.3	81
45	Understanding perceived color through gradual spectroscopic variations in electrochromism. Indian Journal of Physics, 2019, 93, 927-933.	1.8	14
46	Improved field emission from appropriately packed TiO2 nanorods: Designing the miniaturization. Superlattices and Microstructures, 2019, 126, 1-7.	3.1	16
47	Possible origin of ferromagnetism in antiferromagnetic orthorhombic-YFeO3: A first-principles study. Ceramics International, 2018, 44, 13507-13512.	4.8	13
48	Disappearance of dielectric anomaly in spite of presence of structural phase transition in reduced BaTiO3: Effect of defect states within the bandgap. Journal of Applied Physics, 2018, 123, .	2.5	37
49	Structural, optical and electronic properties of RFeO3. Ceramics International, 2018, 44, 8344-8349.	4.8	51
50	TiO <sub>2</sub> –Co <sub>3</sub> O <sub>4</sub> Core–Shell Nanorods: Bifunctional Role in Better Energy Storage and Electrochromism. ACS Applied Energy Materials, 2018, 1, 790-798.	5.1	97
51	Polypyrrole–vanadium oxide nanocomposite: polymer dominates crystallanity and oxide dominates conductivity. Applied Physics A: Materials Science and Processing, 2018, 124, 1.	2.3	7
52	Generalisation of phonon confinement model for interpretation of Raman line-shape from nano-silicon. Advances in Materials and Processing Technologies, 2018, 4, 227-233.	1.4	6
53	Spectroscopic Evidence of Phosphorous Heterocycle–DNA Interaction and its Verification by Docking Approach. Journal of Fluorescence, 2018, 28, 373-380.	2.5	5
54	Effect of electron irradiation on the optical properties of SrTiO <sub>3</sub> : An experimental and theoretical investigations. Materials Research Express, 2018, 5, 036210.	1.6	20

#	Article	IF	CITATIONS
55	Design and development of in-situ temperature dependent diffuse reflectance spectroscopy setup. Journal of Instrumentation, 2018, 13, T11003-T11003.	1.2	15
56	Polythiophene -viologen bilayer for electro-trichromic device. Solar Energy Materials and Solar Cells, 2018, 188, 249-254.	6.2	64
57	Porous Silicon's fractal nature revisited. Superlattices and Microstructures, 2018, 120, 141-147.	3.1	14
58	Diffuse reflectance spectroscopy: An effective tool to probe the defect states in wide band gap semiconducting materials. Materials Science in Semiconductor Processing, 2018, 86, 151-156.	4.0	88
59	Studies on structural and optical gap tunability in α-(Ga Cr(1-))2O3 solid solutions. Journal of Alloys and Compounds, 2018, 766, 876-885.	5.5	5
60	Mesoporous Nickel Oxide (NiO) Nanopetals for Ultrasensitive Glucose Sensing. Nanoscale Research Letters, 2018, 13, 16.	5.7	73
61	Tent-Shaped Surface Morphologies of Silicon: Texturization by Metal Induced Etching. Silicon, 2018, 10, 2801-2807.	3.3	8
62	Synthesis and characterization of RFeO <sub>3</sub> : experimental results and theoretical prediction. Advances in Materials and Processing Technologies, 2018, 4, 558-572.	1.4	8
63	Quantifying the Short-Range Order in Amorphous Silicon by Raman Scattering. Analytical Chemistry, 2018, 90, 8123-8129.	6.5	47
64	Organic Nanostructures on Inorganic Ones: An Efficient Electrochromic Display by Design. ACS Applied Nano Materials, 2018, 1, 3715-3723.	5.0	37
65	Study of Porous Silicon Prepared Using Metal-Induced Etching (MIE): a Comparison with Laser-Induced Etching (LIE). Silicon, 2017, 9, 483-488.	3.3	30
66	Interfacial redox centers as origin of color switching in organic electrochromic device. Optical Materials, 2017, 66, 65-71.	3.6	45
67	Spectral Anomaly in Raman Scattering from p-Type Silicon Nanowires. Journal of Physical Chemistry C, 2017, 121, 5372-5378.	3.1	39
68	Live spectroscopy to observe electrochromism in viologen based solid state device. Solid State Communications, 2017, 261, 17-20.	1.9	21
69	An insight of spirooxindole-annulated thiopyran – DNA interaction: spectroscopic and docking approach of these biological materials. Advances in Materials and Processing Technologies, 2017, 3, 339-352.	1.4	1
70	Evidence of bovine serum albumin-viologen herbicide binding interaction and associated structural modifications. Journal of Molecular Structure, 2017, 1139, 447-454.	3.6	7
71	Room-Temperature Magneto-dielectric Effect in LaGa <sub>0.7</sub> Fe <sub>0.3</sub> O <sub>3+γ</sub> ; Origin and Impact of Excess Oxygen. Inorganic Chemistry, 2017, 56, 3809-3819.	4.0	14
72	Significant field emission enhancement in ultrathin nano-thorn covered NiO nano-petals. Journal of Materials Chemistry C, 2017, 5, 9611-9618.	5.5	28

#	Article	IF	CITATIONS
73	Synthesis of Conducting Polypyrrole-Titanium Oxide Nanocomposite: Study of Structural, Optical and Electrical Properties. Journal of Inorganic and Organometallic Polymers and Materials, 2017, 27, 257-263.	3.7	26
74	Importance of frequency dependent magnetoresistance measurements in analysing the intrinsicality of magnetodielectric effect: A case study. Journal of Applied Physics, 2017, 122, .	2.5	8
75	Strain control of Urbach energy in Cr-doped PrFeO3. Applied Physics A: Materials Science and Processing, 2017, 123, 1.	2.3	53
76	Electronic and optical properties of BaTiO3 across tetragonal to cubic phase transition: An experimental and theoretical investigation. Journal of Applied Physics, 2017, 122, .	2.5	95
77	Fast electrochromic display: tetrathiafulvalene–graphene nanoflake as facilitating materials. Journal of Materials Chemistry C, 2017, 5, 9504-9512.	5.5	55
78	Ecofriendly gold nanoparticles – Lysozyme interaction: Thermodynamical perspectives. Journal of Photochemistry and Photobiology B: Biology, 2017, 174, 284-290.	3.8	22
79	Amplification or cancellation of Fano resonance and quantum confinement induced asymmetries in Raman line-shapes. Physical Chemistry Chemical Physics, 2017, 19, 31788-31795.	2.8	36
80	Construction of well aligned highly dense Cobalt nanoneedles for efficient device application. Advances in Materials and Processing Technologies, 2017, 3, 627-631.	1.4	2
81	Effect of Mn doping on dielectric response and optical band gap of LaGaO <sub>3</sub> . Advances in Materials and Processing Technologies, 2017, 3, 539-549.	1.4	3
82	Phase Transformation and Optical Properties of Annealed Hydrothermally Synthesized ZnO/ZnCr <sub>2</sub> O <sub>4</sub> Nanocomposites. International Journal of Applied Ceramic Technology, 2016, 13, 912-919.	2.1	7
83	Probing structural distortions in rare earth chromites using Indian synchrotron radiation source. Indian Journal of Physics, 2016, 90, 1347-1354.	1.8	16
84	Fe doped LaGaO <sub>3</sub> : good white light emitters. RSC Advances, 2016, 6, 100230-100238.	3.6	35
85	Observation of room temperature magnetodielectric effect in Mn-doped lanthanum gallate and study of its magnetic properties. Journal of Materials Chemistry C, 2016, 4, 10876-10886.	5.5	17
86	Raman spectroscopy for study of interplay between phonon confinement and Fano effect in silicon nanowires. Journal of Raman Spectroscopy, 2016, 47, 283-288.	2.5	43
87	Role of metal nanoparticles on porosification of silicon by metal induced etching (MIE). Superlattices and Microstructures, 2016, 94, 101-107.	3.1	22
88	Spectroscopic Investigation of well aligned Silicon Nano wires Fabricated by Metal Induced Etching. Materials Today: Proceedings, 2016, 3, 1835-1839.	1.8	2
89	Observation of large dielectric permittivity and dielectric relaxation phenomenon in Mn-doped lanthanum gallate. RSC Advances, 2016, 6, 26621-26629.	3.6	30
90	Possibility of spin-polarized transport in edge fluorinated armchair boron nitride nanoribbons. RSC Advances, 2016, 6, 11014-11022.	3.6	17

#	Article	IF	CITATIONS
91	Interplay between phonon confinement and Fano effect on Raman line shape for semiconductor nanostructures: Analytical study. Solid State Communications, 2016, 230, 25-29.	1.9	42
92	Effect of Hf doping on the structural, dielectric and optical properties of CaCu3Ti4O12 ceramic. Journal of Materials Science: Materials in Electronics, 2016, 27, 5878-5885.	2.2	11
93	Quantum confinement effect in cheese like silicon nano structure fabricated by metal induced etching. AIP Conference Proceedings, 2015, , .	0.4	0
94	Effect of hafnium substitution on the dielectric properties of CaCu3Ti4O12. AIP Conference Proceedings, 2015, , .	0.4	3
95	Room temperature magnetodielectric studies on Mn-doped LaGaO <sub>3</sub> . Materials Research Express, 2015, 2, 096105.	1.6	17
96	Effect of silicon resistivity on its porosification using metal induced chemical etching: morphology and photoluminescence studies. Materials Research Express, 2015, 2, 036501.	1.6	22
97	Determination of the optical gap bowing parameter for ternary Ni <sub>1â^'x</sub> Zn <sub>x</sub> O cubic rocksalt solid solutions. Dalton Transactions, 2015, 44, 14793-14798.	3.3	33
98	Half-metallicity in armchair boron nitride nanoribbons: A first-principles study. Solid State Communications, 2015, 212, 19-24.	1.9	16
99	Effect of oxygen partial pressure on properties of asymmetric bipolar pulse dc magnetron sputtered TiO_2 thin films. Applied Optics, 2015, 54, 3817.	2.1	9
100	Stability analysis of zigzag boron nitride nanoribbons. AIP Conference Proceedings, 2015, , .	0.4	0
101	Origin of photoluminescence from silicon nanowires prepared by metal induced etching (MIE). AIP Conference Proceedings, 2015, , .	0.4	1
102	Extended x-ray absorption fine structure measurements on asymmetric bipolar pulse direct current magnetron sputtered Ta_2O_5 thin films. Applied Optics, 2015, 54, 6744.	2.1	16
103	Effect of substrate bias and oxygen partial pressure on properties of RF magnetron sputtered HfO2 thin films. Journal of Vacuum Science and Technology B:Nanotechnology and Microelectronics, 2014, 32, 03D104.	1.2	14
104	Large dielectric permittivity and possible correlation between magnetic and dielectric properties in bulk BaFeO3â~Ĩ´. Applied Physics Letters, 2014, 105, .	3.3	37
105	Symmetry of the charge-ordered phases in Pr <sub>0.5</sub> Ca <sub>0.5</sub> MnO <sub>3</sub> . Philosophical Magazine, 2014, 94, 117-124.	1.6	0
106	Qualitative Evolution of Asymmetric Raman Line-Shape for NanoStructures. Silicon, 2014, 6, 117-121.	3.3	59
107	Readdressing the issue of low-temperature resistivity minimum in La0.7Ca0.3MnO3 thin films. Applied Physics A: Materials Science and Processing, 2013, 113, 793-800.	2.3	1
108	Comparison of spectral performance of HfO[sub 2]â^•SiO[sub 2] and TiO[sub 2]â^•SiO[sub 2] based high reflecting mirrors. , 2013, , .		0

#	Article	IF	CITATIONS
109	Crystallographic phase control of TiO2 in thin films deposited by asymmetric bipolar pulsed DC sputtering. , 2012, , .		1
110	Simulation of thickness and optical constants from transmission spectrum of thin film by envelope method: Practical constraints and their solution. , 2012, , .		1
111	Deposition and characterization of titania–silica optical multilayers by asymmetric bipolar pulsed dc sputtering of oxide targets. Journal Physics D: Applied Physics, 2010, 43, 045302.	2.8	11
112	Possible origin of photoconductivity in La0.7Ca0.3MnO3. Journal of Applied Physics, 2010, 107, 023709.	2.5	6
113	Effect of iron doping on electrical, electronic and magnetic properties of La0.7Sr0.3MnO3. Journal Physics D: Applied Physics, 2009, 42, 185410.	2.8	37
114	Locating the normal to relaxor phase boundary in Ba(Ti1â^'xHfx)O3 ceramics. Materials Research Bulletin, 2008, 43, 1761-1769.	5.2	19
115	Possible origin of electronic phase separation in La0.7Ca0.3MnO3. Journal of Applied Physics, 2008, 104, ·	2.5	6
116	Strain-induced first-order orbital flip transition and coexistence of charge-orbital ordered phases in <mml:math <br="" xmlns:mml="http://www.w3.org/1998/Math/MathML">display="inline"&gt;<mml:mrow><mml:msub><mml:mrow><mml:mtext>Pr</mml:mtext></mml:mrow><mml:mrow Physical Review B, 2008, 78, .</mml:mrow </mml:msub></mml:mrow></mml:math>	3.2 ∨> <mml:m< td=""><td>n&gt;0.5</td></mml:m<>	n>0.5
117	Study of the relaxor behavior in BaTi1â^'xHfxO3 (0.20≤â‰9.30) ceramics. Solid State Sciences, 2007, 9, 1054-1060.	3.2	15
118	Strain induced coexistence of monoclinic and charge ordered phases inLa1â^'xCaxMnO3. Physical Review B, 2006, 74, .	3.2	41
119	Crossover from classical to relaxor ferroelectrics in BaTi1â^'xHfxO3ceramics. Journal of Physics Condensed Matter, 2006, 18, 3455-3468.	1.8	43
120	The contribution of grain boundary and defects to the resistivity in the ferromagnetic state of polycrystalline manganites. Journal of Magnetism and Magnetic Materials, 2006, 306, 60-68.	2.3	10
121	Electron diffraction evidence of charge-ordering at room-temperature in La1â^'xCaxMnO3 (0.55â‰ <b>¤</b> â‰ <b>9</b> .67). Solid State Communications, 2006, 137, 158-161.	1.9	5
122	Ferroelectric relaxor behavior in hafnium doped barium-titanate ceramic. Solid State Communications, 2006, 138, 331-336.	1.9	85
123	Powder X-ray diffraction and Rietveld analysis of La <sub>1â^'<i>x</i></sub> Ca <sub><i>x</i></sub> MnO <sub>3</sub> (0< <i>X</i> <1). Powder Diffraction, 2006, 21, 40-44.	0.2	26
124	Phase separation scenario in Ba doped LaMnO3. Physica Status Solidi C: Current Topics in Solid State Physics, 2004, 1, 3623-3627.	0.8	1